THE EFFECT OF MO AND/OR C ADDITION ON MICROSTRUCTURE AND PROPERTIES OF TIAL ALLOYS

CHLUPOVÁ Alice[1], KRUML Tomáš[2], ROUPCOVÁ Pavla[1],
HECZKO Milan[1], OBRTLÍK Karel[1], BERAN Přemysl[3]

[1] *Institute of Physics of Materials, AS CR, Zizkova 22, 616 62 Brno, Czech Republic, EU, chlupova@ipm.cz*

[2] *CEITEC, Institute of Physics of Materials, AS CR, Zizkova 22, 616 62 Brno, Czech Republic*

[3] *Nuclear Physics Institute, AS CR, 25068 Rez, Czech Republic*

Abstract

Cast TiAl alloys with high Nb content are subject of extensive research with the aim to develop material with low density, good corrosion resistance and high strength at elevated temperatures. Disadvantage of their broad applications is restricted workability, machinability and low fracture toughness especially at room temperature. Improvement of properties of TiAl based materials can be achieved by tailoring the microstructure by modification of chemical composition. For this purpose 5 types of TiAl alloys with 7 % of Nb were prepared having variable content of Mo and/or C. Addition of Mo and/or C resulted in three types of microstructure and different phase composition. All modified alloys contain colonies consisting of thin lamellae of α and γ phases sometimes complemented by γ and/or β phase at the grain boundaries. Variable microstructure and phase composition resulted in differences in mechanical behaviour. The most promising tensile properties at both room and elevated temperature were observed for alloy doped with 2 % of Mo having the mixed microstructure containing β phase and for alloy doped with 0.5 % of C with nearly lamellar microstructure without β phase. 2Mo alloy exhibited reasonably good ductility while 0.5C alloy reached the highest tensile strength. Also low cycle fatigue behaviour of these two materials was the best of all five materials under investigation. Fatigue deformation characteristics were better in the case of 2Mo alloy while 0.5C alloy exhibited higher cyclic stresses. Fracture mechanisms were determined using fractographic analysis. The major fracture mode of all alloys was trans-lamellar.

Keywords: TiAl, microstructure, mechanical properties, effect of alloying, fractography

1. INTRODUCTION (6 PAGES, 20 MB)

Third generation of TiAl alloys contains high amount of Nb which results in significant strengthening, creep resistance and good oxidation resistance [1-3]. Improvement of mechanical and/or technological properties depends on the refinement of microstructure and on the presence of β phase. Strengthening controlled by microstructure refinement can be connected with the higher content of α phase stabilizing element like C, while β phase introduced into material by addition of beta stabilizing elements like Nb and Mo is responsible for higher ductility but lower mechanical properties at elevated temperature [4-6].

The aim of this research was to modify chemical composition in order to study the effect of Mo and/or C addition on the microstructure, phase composition and mechanical properties. Therefore, five types of TiAl alloys having 7 % of Nb were prepared with variable content of Mo and/or C. Microstructure and phase composition varied and as a consequence the differences in mechanical properties both at RT and elevated temperature were observed. On the basis of tensile and fatigue tests results, the most promising material can be chosen. Fractographic analysis was performed in order to identify the mechanism of fracture in dependence on microstructure and phase composition.

2. EXPERIMENT

Five types of TiAl alloys were prepared with 7 at % Nb and variable content of Mo and C (see ***Table 1***). Ingots were HIP treated at (1260 ± 10) °C for 4 hrs under pressure (170 ± 5) MPa in order to reduce porosity and lower the scatter in mechanical properties.

Table 1: Chemical composition of individual ingots and phase composition evaluated using neutron diffraction [7] and x-ray diffraction method. *Values influenced by texture.

								Phase composition [vol. %]					
	Chemical composition [at. %]							Neutron diffraction			XRD		
	Al	Nb	Ni	Si	Mo	C	Ti	α-Ti_3Al	β-TiAl	γ-TiAl	α-Ti_3Al	β-TiAl	γ-TiAl
TiAl7Nb 2Mo	46	7	0.2	0.1	2	-	bal.	3.4	14.6	82.0	3.6	15.7	80.7
TiAl7Nb 0.2C	46	7	0.2	0.1	-	0.2	bal.	15.0	-	85.0	10*	4.9*	85.1*
TiAl7Nb 0.5C	46	7	0.2	0.1	-	0.5	bal.	20.0	-	80.0	6.1*	0.7*	93.2*
TiAl7Nb 2Mo0.2C	46	7	0.2	0.1	2	0.2	bal.	9.2	8.7	82.1	8.3	9.1	82.6
TiAl7Nb 2Mo0.5C	46	7	0.2	0.1	2	0.5	bal.	12.1	6.8	81.1	11.5	6.5	82

Cylindrical specimens were cut from ingots by electric spark discharge method and machined to a final shape with gauge diameter 5 mm and gauge length 8 mm for testing at RT and gauge diameter 5 mm and gauge length 15 mm for testing at elevated temperatures. Surface of specimens was mechanically ground and electrolytically polished to avoid big scatter of measured data. Microstructural and fractographic studies were performed using scanning electron microscope Tescan LYRA 3 XMH FEG/SEM.

Tensile and fatigue properties measurement was conducted on MTS 810 servohydraulic testing machine with Teststar IIs digital control unit. Tensile tests were performed with strain rate 10^{-4} s^{-1}. Fully reversed total axial strain-controlled LCF tests were conducted at constant strain rate $2x10^{-3}$ s^{-1}. High temperature tests (700 °C, 750 °C and 800 °C) were performed in air using resistance heating furnace. MTS extensometers were used to measure deformation at room and elevated temperatures.

Phase composition was determined using neutron diffraction experiments [7] and by means of x-ray diffraction. X-ray powder diffraction (XRD) was performed using Co Kα radiation. Qualitative analysis was yielded by the HighScore software and the JCPDS PDF-4 database. BGMN structural models based on the ICSD database were used for the quantitative analysis of XRD patterns.

3. RESULTS AND DISCUSSION

3.1. Microstructure and phase composition

The microstructure of all ingots consists of two or three phases: ordered tetragonal γ phase - TiAl ($L1_0$ structure; space group P4/mmm); ordered hexagonal α phase - Ti_3Al ($D0_{19}$ structure; space group P63/mmc) and cubic β phase - TiAl (with A2 disordered or B2 ordered structure; space group Pm-3m). Results concerning phase composition are given in ***Table 1***. Data evaluated using XRD were compared with results from neutron diffraction method [7]. In the case of the material containing Mo (2Mo, 2Mo0.2C and 2Mo0.5C), XRD results are comparable to the neutron diffraction method. For alloys containing only C (0.2C and 0.5C) the phase composition data by XRD are considerably different from those obtained by neutron diffraction, indicating presence of certain amount of β phase even if C is element suppressing formation of this phase. It can be related to strong texture of measured samples which affects the precision of XRD measurements.

Three typical microstructures for individual alloys were observed (see ***Fig. 1***):

The microstructure of 2Mo alloy (see ***Fig. 1 a***) can be characterised as a mixed one consisting of lamellar colonies of α+γ phase surrounded by mixture of γ grains and β phase with very irregular and usually elongated shape (white colour phase). The amount of β phase is approx. 15 % which is the highest from all studied materials. The α phase (approx. 3 %) is present in the form of rather thick lamellae. The mean

spacing between two consecutive lamellae is the highest from all observed materials. It seems that some of the α lamellae were partially transformed to β. According to [3], the α to β transformation can be explained by the close chemical composition and instability of the α phase supersaturated by Mo and Nb.

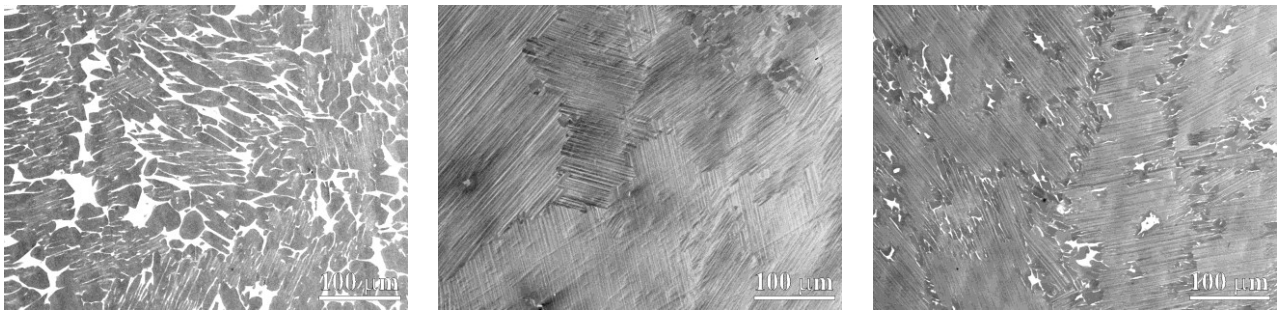

a) b) c)

Fig. 1: Micrographs of TiAl alloys: a) alloy doped with 2 % of Mo, b) with 0.2 % of C, c) with 2% of Mo and 0.5 % of C, (all in BSE mode).

Microstructures for 0.2C alloy (see ***Fig. 1 b***) and for 0.5C alloy are very similar with fully or nearly lamellar structure and well-interlocked grain boundaries. In both alloys lamellar colonies are approximately the same size, nevertheless higher C content results in finer lamellae of α+γ phases. In agreement with neutron diffraction experiments no β phase was observed in microstructure of both materials and only occasionally some γ grains were found at grain boundary or triple junctions (see the right upper corner in ***Fig. 1b***).

An example of the microstructure of 2Mo0.5C alloy is in ***Fig. 1 c***). The microstructure can be described as mixed with uniformly distributed lamellar colonies framed with grains of γ phase sometimes together with β islands inside them. The microstructure of 2Mo0.2C alloy is very similar with approximately the same size of lamellar colonies. The lower content of C in case of 2Mo0.2C results in higher amount of β phase with rather elongated and spiky shapes. The higher content of C in the case of 2Mo0.5C causes refinement of lamella thickness resulting in the lowest inter-lamellar space from all five studied materials.

3.2. Mechanical properties

All materials were subjected to tensile testing at room temperature and at 750 °C. Results are listed in ***Table 2***. Fracture stress and yield stress are high for all materials at both temperatures. The highest values of strength at 750 °C can be ascribed to NL structure of 0.5C alloy. Due to limited plasticity of all alloys the 0.2 % proof stress could be evaluated only for more ductile alloys at 750 °C. In other cases proof stresses Rp0.1, Rp 0.05 and Rp 0.02 were assessed (see ***Table 2***). The highest amount of β phase in 2Mo alloy resulted in rather low strength, nevertheless in the best plastic properties at 750 °C when plastic strain at fracture reached the value of 0.38 %.

Table 2 Tensile properties of five TiAl alloys at RT and 750°C.

	RT				**750 °C**				
	$R_p0.02$ [MPa]	$R_p0.05$ [MPa]	ε_{pf} [%]	σ_f [MPa]	$R_p0.05$ [MPa]	$R_p0.1$ [MPa]	$R_p0.2$ [MPa]	ε_{pf} [%]	σ_f [MPa]
2Mo	467	480	0.058	485	380	406	441	0.38	485
0.2C	498	536	0.085	563	-	-	-	-	-
0.5C	610	-	0.026	619	548	590	628	0.24	636
2Mo0.2C	531	-	0.032	538	427	454	483	0.28	499
2Mo0.5C	-	-	0.008	601	525	-	-	0.17	524

Plot of tensile stress-strain curves for two most promising materials (the most plastic 2Mo alloy and strongest 0.5C alloy) at room and elevated temperature is shown in ***Fig. 2***.

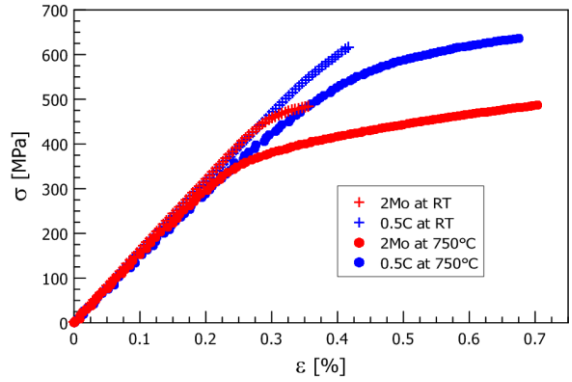

Fig. 2: Tensile stress-strain curves for two TiAl alloys (2Mo and 0.5C).

Fatigue behaviour of TiAl alloys was studied both at RT and 750 °C. A short-cut procedure was applied to obtain cyclic stress-strain curves (CSSC). In cyclic loading, all materials exhibited rather brittle behaviour even at high temperature. The most promising fatigue properties at 750 °C were observed in the case of 2Mo and 0.5C alloys (see ***Fig. 3a***). These alloys show the highest level of cyclic plasticity. Material with 0.5C having NL microstructure with the highest amount of α phase also exhibits the highest cyclic stress response at 750 °C. The stress amplitude as a function of the plastic strain amplitude is shown in ***Fig. 3b*** for 750 °C. The highest level of plastic deformation in these cyclic stress-strain curves C is reached in the case of 2Mo alloy which contains the highest amount of β phase in the microstructure. The plot of the stress amplitude versus the number of cycles shows cyclic softening during cycling of all alloys at 750 °C usually with strain amplitude equal approximately to 0.27 % and higher. At room temperature, cyclic softening starts at higher strain amplitudes (0.33 %) in comparison with tests at 750 °C. This behaviour differs from that observed in the case of TiAl alloy with 8% of Nb without additional doping [8] where no cyclic softening was observed below 800°C.

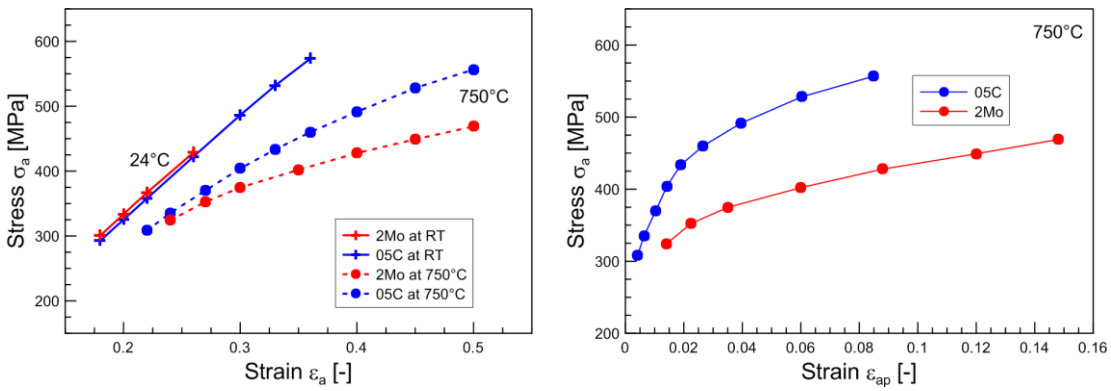

a) b)

Fig. 3: a) Plot of the stress amplitude σ_a vs the total strain amplitude ε_a for two selected alloys (2Mo and 0.5C) tested at RT and 750 °C. b) Cyclic stress-strain curves for 2Mo and 0.5C alloys tested at 750 °C.

3.3. Fractography

Thorough analysis of fracture surfaces of all specimens after tensile and fatigue tests to fracture shows very similar appearance. No significant differences between tensile and fatigue fracture were noticed. This can be due to application of short-cut procedure to obtain CSSC, which probably affects fatigue crack initiation.

When lamellar colonies are present in the microstructure then also fracture modes reflects it. Generally, two fracture modes were observed: 1) inter-lamellar mode appears when a crack grows along lamellar interfaces leaving flat facets on the surface (see ***Fig. 4a***) and 2) trans-lamellar fracture appears in case that cracks grow perpendicularly to the lamellar interfaces. In the second mode, two following characteristic features can be found on the surface: 1) steps with different thickness corresponding to the lamellae thickness (see ***Fig. 4b***) and 2) cleavage facets, where the fracture goes through lamellae. An individual lamella can be distinguished only in phase contrast (see ***Fig. 4c***).

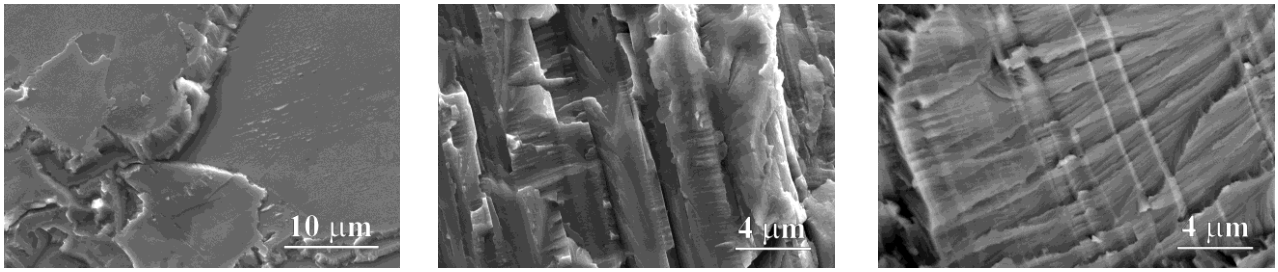

a) b) c)

Fig. 4: a) Fracture surface with inter-lamellar fracture (SE mode), b) trans-lamellar fracture with steps corresponding to lamellae (SE), c) trans-lamellar fracture with cleavage facets and river-like ridges (BSE).

In our study, the inter-lamellar fracture was observed only occasionally and predominantly in case of 0.2C alloy. Comparison of fracture mechanisms for two alloys 0.2C and 0.5C (without β phase) revealed that despite of similar fully or nearly lamellar microstructure (see ***Fig. 1b***) the 0.2C alloy exhibits higher volume of inter-lamellar fracture indicating the fracture stress at RT approx. 50 MPa lower than that in case of 0.5C alloy. The trans-lamellar fracture is more energetically demanding which results in the highest fracture stress of 0.5C alloy even at 750°C.

The β phase is usually present in the microstructure in the form of islands surrounded by gamma phase at lamellar colony boundaries or triple junctions (see ***Fig. 1 a,c***). Fractographic observation in 2Mo, 2Mo0.2C and 2Mo0.5C alloys revealed that fractures initiate predominantly in areas rich in β and γ phase. An example of this type of initiation site is in ***Fig. 5a***.

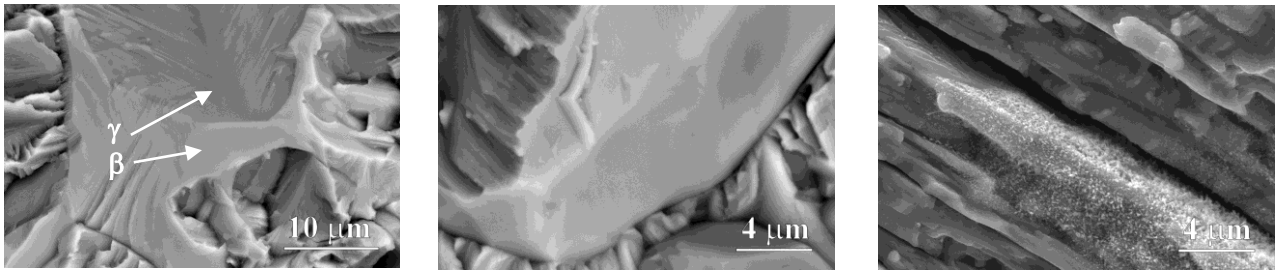

a) b) c)

Fig. 5: a) Crack initiation site in β phase (brighter colour) surrounded by γ phase (BSE), b) inter-granular fracture caused by increased temperature (BSE), c) oxidation at 750 °C and delamination between two areas with trans-lamellar fracture with inter-lamellar secondary cracking (SE).

Investigation of differences between fracture mechanisms at RT and 750°C showed the higher amount of inter-granular fracture after loading at 750 °C (see ***Fig. 5b***). Oxidation products were present on the fracture surface after loading at 750 °C - see trans-lamellar fracture in ***Fig. 5c***.

Fracture and crack growth are often very instable processes and it is very profitable, when the most energy consumption is related to creation of crack branching or secondary failure. In case of lamellar structure, the crack branching can be in the form of the secondary inter-lamellar fracture (***Fig. 5c***). The highest amount of

these features was observed on the fracture surface of 0.5C alloy. It is in agreement with the high fracture resistivity of this material.

CONCLUSIONS

Microstructure and phase composition of the cast TiAl alloy with 7 % of Nb with modification of chemical composition using variable content of C and/or Mo were studied. Five types of TiAl alloys exhibited different phase composition and three types of microstructure containing colonies consisting of thin lamellae of α and γ phases sometimes complemented by γ and/or β phase at the grain boundaries

Variable microstructure and phase composition resulted in differences in tensile and fatigue behaviour. The most promising tensile properties at both room and elevated temperature were observed for alloy doped with 2 % of Mo containing 15% of β phase and for lamellar material with 0.5 % of C without β phase. 2Mo alloy exhibited reasonably good ductility while 0.5C alloy reached the highest tensile strength. The best fatigue stress-strain characteristics were observed for 2Mo and 0.5C alloys. The level of cyclic plasticity was higher in case of 2Mo alloy while 0.5C alloy exhibited more pronounced cyclic stress response.

Fracture mechanisms were determined; the major fracture mode of all alloys is trans-lamellar. In the case of high temperature loading, the presence of inter-granular fracture and oxidation was observed. Fracture surfaces after tensile and fatigue loading were found very similar.

ACKNOWLEDGEMENTS

Research was supported by the projects of the Czech Science Foundation 107/11/0704 and 15-08826S. Also the project RVO 68081723 of Academy of Sciences of the Czech Republic is acknowledged. The research was partially conducted in CEITEC research infrastructure supported by the project CZ.1.05/1.1.00/02.0068.

REFERENCES

[1] APPEL F., OEHRING M., WAGNER R.: Novel design concepts for gamma-base titanium aluminide alloys, Intermetallics, Vol. 8, 2000, pp. 1283-1312.

[2] HUANG Z.W., VOICE W.E., BOWEN P.: Thermal stability of Ti–46Al–5Nb–1W alloy, Materials Science and Engineering, Vol. A329–331, 2002, pp. 435–445.

[3] IMAEV V. M., IMAEV R. M., OLENEVA T. IKHISMATULLIN., T. G.: Microstructure and Mechanical Properties of the Intermetallic Alloy Ti–45Al–6(Nb, Mo)–0.2B, The Physics of Metals and Metallography, Vol. 106, No. 6, 2008, pp. 641–648.

[4] CHEN Y., NIU H., KONG F., XIAO S.: Microstructure and fracture toughness of a β phase containing TiAl alloy, Intermetallics, Vol. 19, 2011, pp. 1405-1410.

[5] LIU B., LIU Y., LI Y.P., ZHANG W., CHIB A.: Thermomechanical characterization of β-stabilized Ti-45Al-7Nb-0.4W-0.15B alloy, Intermetallics, Vol. 19, 2011, pp. 1184-1190.

[6] PERDRIX F., TRICHET M.F., BONNENTIEN J.L., CORNET M., BIGOT J.: Relationships between interstitial content, microstructure and mechanical properties in fully lamellar Ti–48Al alloys, with special reference to carbon, Intermetallics, Vol. 9, 2001, pp. 807–815.

[7] BERAN P., PETRENEC M., HECZKO M., SMETANA B., ZALUDOVA M., SMID M., KRUML T., KELLER L.: In-situ neutron diffraction study of thermal phase stability in a g-TiAl based alloy doped with Mo and/or C, Intermetallics, Vol. 54, 2014, pp. 28-38.

[8] KRUML T., CHLUPOVÁ A., OBRTLÍK K.: Cyclic deformation of a modern TiAl alloy at high temperatures, Advanced Materials Research, Vol. 891-892, 2014, pp. 1131-1136.